

Sensory Redundant Parallel Mobile Mechanism

Shraga Shoval and Moshe Shoham*

Department of Industrial Engineering & Management, Academic College of Judea and Samaria, Ariel.,

*Faculty of Mechanical Engineering, Technion, Haifa, Israel

Abstract

This paper presents a novel design for a mobile robot based on the kinematics of parallel mechanisms. The robot consists of 3 legs, each equipped with an asynchronous driving unit. The legs are connected to the driving units with spherical joints and to the upper plate with a revolute joint. Three additional encoders, attached to the upper revolute joints provide redundant data. This data is used by a kinematic model for accurate estimation of the robot's configuration and position in space, even in rough terrains, where conventional odometry fails. Simulation results show the advantages of the design, and suggest a method for detection of irregularities of surfaces in unknown environments.

1. Introduction

Parallel manipulators consist of several actuators connected in parallel to a base and a moving platform. The structure of parallel manipulators makes them particularly suitable for applications where accuracy, rigidity and high payload – to – weight ratio are important, since their stiffness and dynamic performance are largely superior to those achieved with conventional serial architectures. The maneuverability as well as rigidity and accuracy are functions of the number of legs, dimensions of the mechanism, and the type of joints between the plates and the legs. The basic conceptual mechanics is known as the Stewart Platform [Stewart, 1965] (even though an earlier design was suggested by Gough). Since then, many manipulators were developed based on this mechanism [Fitcher and MacDowel 1980, Hunt 1983, Yang and Lee 1984, Fichter 1986, Kohli et. al. 1988, Hudgens and Tesat 1988, Tsai and Tahmasebi 1983]. Fig. 1 shows some typical parallel mechanisms named according to the number of joints at each platform.

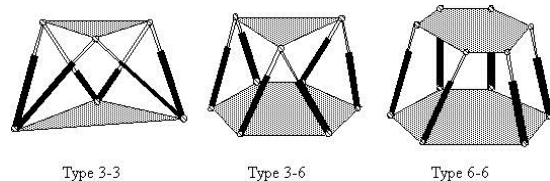


Figure 1: Three types of parallel mechanisms

A major drawback of parallel robots is their limited working envelope that makes them unsuitable for a wide variety of applications. To overcome this shortcoming, several researchers have suggested using mobile joints between the legs and the stationary platform, turning the mechanism into a semi-mobile robot. Such a mechanism developed by Ben Horin and Shoham [1994], is shown in Fig. 2. It consists of the following components: three links of fixed length having a spherical joint on one end and a revolute joint on the other end, three actuators which move planarly on a stationary platform and an output platform having six degrees-of-freedom (DOF).

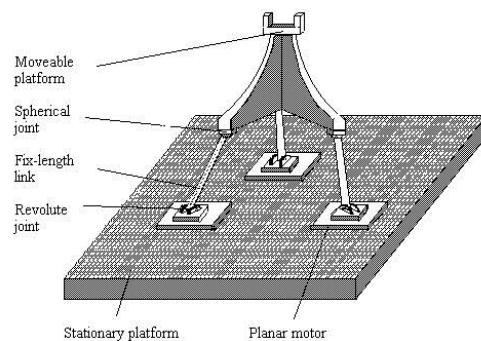


Figure 2: Semi-mobile parallel mechanism [Ben Horin and Shoham, 1996]

To further increase mobility, Ben Horin and Shoham [1999, 2000] suggest a more flexible design. This mechanism, shown in figure 3, is based on 3 inflatable legs, an upper platform and 3 asynchronous driving units for the three legs. This mechanism turns the robot to an autonomous agent, with theoretically unlimited workspace. The upper joint of each leg is a

revolute joint, while the lower joint, which connects the leg to the driving unit, is a spherical joint. This configuration offers six DOF for the upper plate where the control parameters are the positions (X,Y) of the three driving units. The mechanism is designed for applications that require a light weight and easy deployable robot. Given the required trajectory for the TCP (6 parameters) the inverse kinematics model can generate the required path of each driving unit, subject to its non-holonomic constraints.



Figure 3: The inflatable mobile parallel robot [Ben Horin and Shoham, 2000]

The robot's position can be determined either by absolute methods (triangulation, map matching GPS etc.) or by a relative method (i.e. odometry). In order to achieve maximum autonomy, the use of absolute positioning should be restricted to the beginning of motion and to the instances where relative positioning is not sufficiently accurate. In this paper we propose a modified kinematic design of the parallel mobile robot which allows for improved position estimate based on odometry, and also improves both the accuracy of the robot and its robustness to external disturbances due to slippage of the driving wheels, uneven surfaces, bumps holes etc. In Section 2 we describe the problem of dead reckoning for the parallel mobile robot. Section 3 details the mathematical and geometrical model of the robot. Section 4 shows simulation results of the robot operating under various motion

constraints and Section 5 gives concluding remarks.

2. Dead reckoning for parallel mobile mechanism

Fig. 4 is a schematic description of the parallel mobile mechanism. The upper plate is connected to each of the three legs with revolute joints. These three legs are driven by three asynchronous units that are connected to the legs with spherical joints. Controlled motion of the three driving units determines the pose (position and orientation) of the upper plate.

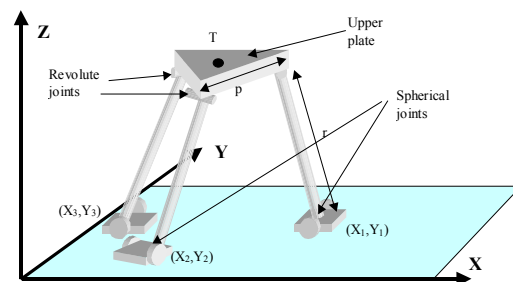


Figure 4: Schematic description of the mobile parallel mechanism

Given the coordinates of point T on the upper plate, the position of the three driving units $(X_1, Y_1, X_2, Y_2$ and $X_3, Y_3)$ is determined by the inverse kinematics model (see Ben-Horin et. al. [2000] for a detailed solution of the path when non-holonomic constraints are considered). The lateral position of the driving units can then be determined either by odometry or triangulation. Using triangulation for each driving unit requires preparation of the surroundings that also restricts the motion space. Also, triangulation can become complex, due to possible interference of the legs with the triangulation procedure by obstructing the beacons.

Using odometry, on the other hand, provides full autonomy for the robot, with no preparation or pre-knowledge of the environment. However, odometry generates unbounded errors that reduce its effectiveness over relatively long travel ranges. The presence of bumps, holes, or slippage in one or more of the driving wheels can create unpredictable errors that increase with travel distance. For example, if one of the driving units is subjected to angular error of 1° (due to slippage of one driving wheel), a travel of 90ft generates a lateral error of 1.5ft in the position of the upper plate. This error also affects the orientation of the upper plate as shown in

Fig. 5. In this example the limbs' length is 5ft, and the upper plate is an equilateral triangle of 5ft. At the end of the 90ft trajectory the upper plate has an angular error of 2.62° . This error increases with travel until the robot stops, reaches a singularity or other undesirable configuration.

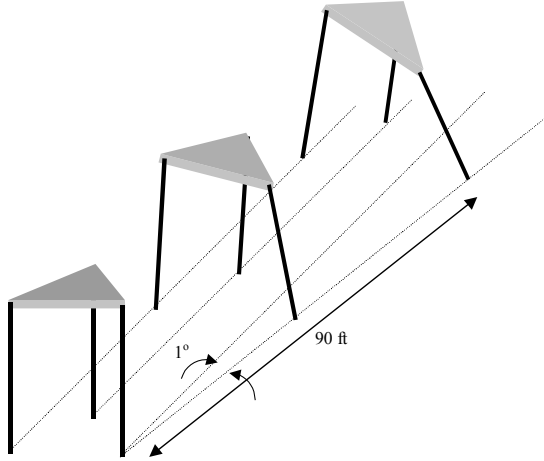


Figure 5: The effect of 1° angular offset on the robot configuration

To determine the accurate configuration of the upper plate, the absolute position of each driving unit, as well as the direct kinematic model are required. Tahmasebi and Tsai [1994] show that the above parallel mechanism has 16 possible direct kinematic solutions, which require extensive computational effort. Furthermore, determining the absolute position of each driving unit is subject to odometric errors and cannot provide a reliable position estimate.

In the following section we propose a new approach to the design and motion control of the parallel mobile robot that relies on odometric data and on additional measurements taken from on board encoders. It requires minor mechanical modifications to the original design, and suggests a geometric model for the new design. This approach does not require preliminary setup of the environment, allowing a full autonomous motion. Furthermore, our approach detects odometric errors in real time, and suggests a fast procedure to correct these errors before affecting the overall robot configuration.

3. The mechanical and geometric model of the modified design

Fig. 6 shows schematic description of the mobile parallel robot already shown in Fig. 4. However, this design includes 3 additional encoders attached to the upper revolute joints, to measure the rotation angle between the upper plate and the legs. These angles are η_1, η_2, η_3 corresponding to the three legs 1, 2 and 3.

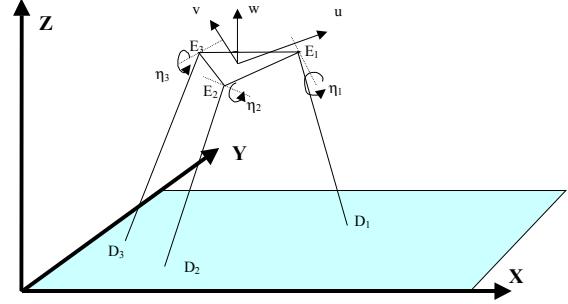


Figure 6: The modified design of the robot

The position of the three drive units ($U_1, V_1, W_1, U_2, V_2, W_2$ and U_3, V_3, W_3) can be derived in the U-V-W coordinate system (attached to the center of the upper plate) according to Eq (1-3) [Tahmasebi and Tsai, 1994]:

$$U_i = r \cos \alpha_i \cos \eta_i + \frac{p}{\sqrt{3}} \cos \alpha_{ii} \quad \text{Eq (1)}$$

$$V_i = r \sin \alpha_i \cos \eta_i + \frac{p}{\sqrt{3}} \sin \alpha_i \quad \text{Eq (2)}$$

$$W_i = -r \sin \eta_i \quad \text{Eq (3)}$$

where

$$\alpha_i = \frac{\pi}{2} + (i+1) \frac{2\pi}{3}$$

p – the length of the edge of the equilateral triangle constructing the upper plate.

r – the length of the legs

i – index of the legs in a cyclic order

Based on the position of the drive units as determined in the upper plate coordinate system, the Euclidean distances between the drive units l_1, l_2 and l_3 is given by Eq (4):

$$l_i = \sqrt{(U_{i-1} - U_{i+1})^2 + (V_{i-1} - V_{i+1})^2 + (W_{i-1} - W_{i+1})^2} \quad \text{Eq (4)}$$

(i – in cyclic order)

Returning to the world coordinate system (X, Y, Z), the position of the drive units is determined by the odometric system where

$D_1=(X_1,Y_1,Z_1)$, $D_2=(X_2,Y_2,Z_2)$ and $D_3=(X_3,Y_3,Z_3)$. The distances between the drive units can also be derived according to Eq (5):

$$l_i = \sqrt{(X_{i-1} - X_{i+1})^2 + (Y_{i-1} - Y_{i+1})^2 + (Z_{i-1} - Z_{i+1})^2} \quad \text{Eq (5)}$$

If the odometric system is accurate, the distances derived in the upper plate coordinate system in Eq (4) is equal to the distances derived in the world coordinate system according to Eq (5). If, however, these distances are different and assuming that the encoder readings of the revolute angles are accurate, then the odometric calculation is faulty. Before proceeding with the rest of the calculations, let us assume that odometric errors occur with a single driving unit at a time. For example, if the robot is traveling over slippery terrain, the momentary effect is on a single drive unit (the unit that drove over the slippery spot). This assumption is realistic when the sampling rate is fast enough as shown by Borenstein [1995]. In his work, Borenstein shows that the effect of odometric errors on a 4 DOF planner mobile robot can be detected separately for each driving unit, then corrected before the overall robot configuration is affected. According to this assumption, errors in the odometric procedure of each driving unit can be detected and corrected in real time by comparing the distances calculated by the X-Y-Z and U-V-W coordinate systems.

An odometric error in one drive unit affects two distances according to Eq (5). Fig. 7 shows a case where the position of two driving units D_1 and D_2 are accurately determined, but the position of D_3 as determined by odometry has an offset Δl . This offset affects the values of two distances: l_1 (distance between D_1 and D_2) and l_2 (distance between D_1 and D_3). The length of l_3 is not effected by the faulty position estimate of D_3 (see Eq (5)). The real location of drive unit 3 is given by the intersection of the two circles - C_1 and C_2 where the radius for C_1 is $l_1/2$ and for C_2 is $l_2/2$. Given that the centers of these circles - D_1 and D_2 are known, the location of D_3 can be calculated. If the above procedure is performed at relatively short intervals (i.e. every 50 milliseconds) the positions of the three driving units remain accurate. As mentioned, this procedure assumes that there is a single odometric error at a time. In the unlikely event that two (or three) driving units are subjected to odometric errors simultaneously, the proposed procedure cannot be implemented and additional

measures must be taken (i.e. re-calibration of the robot's position).

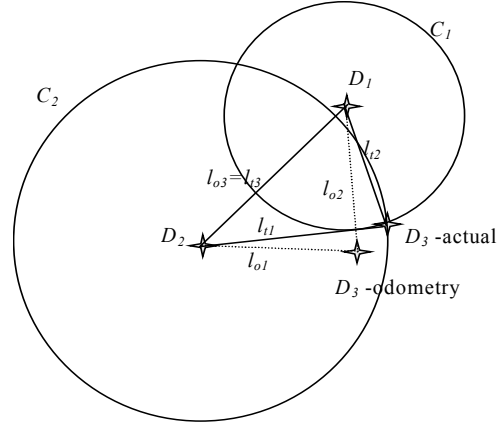


Figure 7: Determining the position of D_3 by the intersection of C_2 and C_1

4. Simulation results

To investigate the validity of our approach, a simulation was developed. The simulation determines the angles between the three legs and the upper platform (η_1, η_2, η_3) based on the actual position of the three driving units (in a real system these angles are measured by the encoders attached to the revolute joints). The simulation then calculates these angles based on the odometric information given by each driving unit. Based on the differences of these calculations the simulation then corrects the estimated position of each driving unit and updates the robot's overall model to determine the position and orientation of the upper platform. A random noise is added to the calculation of the angles η_1, η_2 and η_3 , similar to noise expected from the encoders. The noise in the real system is due to encoder resolution and backlash. In the simulation shown in this section, random noise is in the order of $\pm 1^\circ$. The addition of the $\pm 1^\circ$ ensures that the simulation closely matches the performance expected of a real system.

In the first experiment, an initial odometric error of 2° is introduced to one of the driving units. This error adds a constant value to the initial orientation of that driving unit, resulting in a constant growing lateral error, similar to the example shown in Fig. 5. The robot is traveling for 20m at a speed of 0.66 m/sec with a sampling rate of 20 Hz. As shown in Fig. 8, the odometric path does not detect the initial orientation error

while the path calculated by the algorithm is close to the actual path of the driving unit.

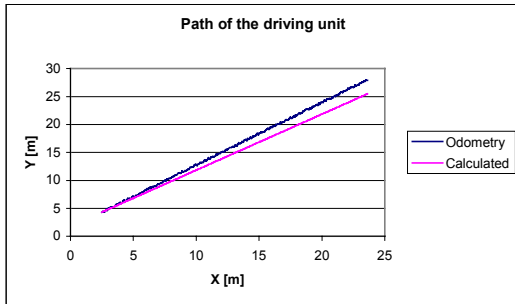
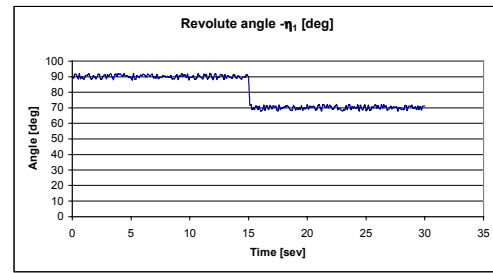


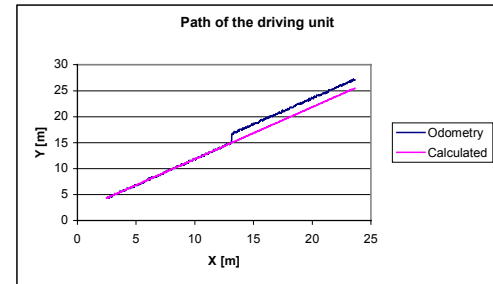
Figure 8: Path of the driving unit subjected to initial orientation error.

In the second simulation, an odometric error is generated after 15 seconds. This causes a lateral error in one of the driving units of 2.5cm into the center of the robot. Such an error can be generated by slippage of the wheels on wet a surface, moving over bumps or by an external disturbance applying an unexpected force on the driving unit. As shown in Fig. 9a, the odometric error is immediately detected by changes in the angle η_i between leg #1 and the upper platform, and the robot's configuration is updated according to that change. Figure 9b shows an estimate of the path of drive unit #1 based on odometry alone, and according to the suggested sensory-redundant kinematic model correction. As shown, odometry does not detect the error in the position of leg #1, while the suggested model detects the odometric error (based on the unexpected changes in η_i) and updates the position of leg #1 to its correct value.

This simulation shows an important feature of the kinematic model. In addition to the detection of the odometric error, the type and source of the error can be predicted. For example, a sudden change in η_i , (as is the case of this experiment) indicates that the odometric error pushed leg #1 into the center of the robot's structure. This might be the case when leg #1 travels over a bump, is pushed inwards by an external force. A sudden increase in η_i indicates that leg #1 is pushed away from the center of the robot, either by external disturbance, slippage, or by traveling over a hole.



a



b

Figure 9: Change in η_i due to odometric error and its effect of the path of the driving unit.

Finally, a simulation where all driving units are subjected to random odometric errors is shown in Fig. 10. This example is typical of motion over uneven terrains (i.e. paved roads, grass, sand etc), where all driving units are continuously subjected to random disturbances. Disturbances cause odometric errors of up to 1 cm/sec for each driving unit. All driving units are subjected to the disturbances simultaneously, causing a maximum lateral error of 1.19 m on the XY plane, and 0.019 m along the YZ plane. The system detects these odometric errors as soon as they occur and updates the robot configuration. If, for example, the robot's mission is to travel along a straight line, these updates can be integrated into the path planning and control system. The control system detects the odometric errors and compensates for them before a significant lateral error is developed.

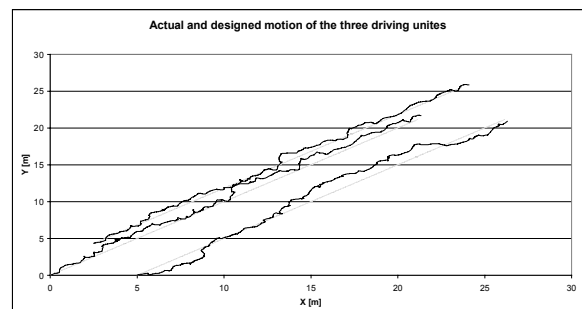


Figure 10: Simulation of random odometric error for three driving units simultaneously

5. Conclusions

A novel design for a mobile robot is presented. The kinematic design combines techniques of parallel mechanisms with conventional wheeled units. The robot consists of three legs, each driven by an asynchronous mechanism connected to the legs with a spherical joint. Each leg is also connected to an upper platform with a revolute joint, resulting in a mobile, six DOF, parallel mechanism. Additional encoders measuring the revolute angle of the upper joints, provide data used by a kinematic model to detect and correct positioning errors generated by odometry. Early detection and correction of odometric errors in each leg prevent significant errors of the upper plate, allowing an autonomous, more accurate and reliable motion even on uneven surfaces, where odometry alone generates unbounded position error.

The features of the kinematic model can be used for identification of irregularities in the environment. For example, when an odometric error is detected in a specific leg (by unexpected changes in the reading of the encoder attached to the upper revolute joint), the source of the odometric error can be determined. Furthermore, the cause of the error, in terms of bumps or holes, inward or outward slippage and the direction of external disturbance, can also be identified.

6. References

1. Ben Horin (Dombiak) P., 1999, "Analysis and Synthesis of an Inflatable Parallel Robot", M.Sc. Thesis, Technion, Haifa.
2. Ben Horin (Dombiak) P., Shoham, M., and Grossman, G., "A Parallel Six Degrees of-Freedom Inflatable Robot," ASME 2000 Mechanism and Robotics Conference, Washington, 2000.
3. Ben Horin R., Shoham M., Djerassi S., 1998, "Kinematics, Dynamics and Construction of a Planary Actuated Robot" Robotics and Computer-Integrated Manufacturing, Vol, 14, No. 2, pp-163-172.
4. Borenstein J., 1995, "Internal Correction of Dead-Reckoning Errors with a Dual-Drive Compliant Linkage Mobile Robot", Journal of Robotics Research, Vol. 12, No. 4, pp. 257-273.
5. Fitcher E.F., 1986, "A Stewart Platform-Based Manipulator: General Theory and Practical Construction", International Journal of Robotics Research, Vol. 5, pp. 157-182.
6. Fitcher E.F., and MacDowel E.D., 1980, "A Novel Design for a Robot Arm", Proceedings International Computer Technology, ASME, New York, pp 250-256.
7. Hudgens J.C., Tesar D., 1988, "A Fully-Parallel Six Degrees-of-Freedom Manipulator: Kinematic and Dynamic Model", Trends and Developments in Mechanisms, Machines and Robotics", Proceedings of the 20th Biennial Mechanism Conference, ASME, New York, Vol. 15, No. 3, pp. 29-37.
8. Hunt K.H., 1983, "Structural Kinematics of In-Parallel-Actuated Robot Arm", ASME Journal of Mechanisms, Transmissions and Automation in Design, Vol. 105, pp. 705-712.
9. Kohli D., Lee S. H., Tsai K. Y., Sandor G. N., 1988, "Manipulator Configuration Based on Rotary-Linear (R-L) Actuators and Their Direct and Inverse Kinematics", ASME Journal of Mechanisms, Transmissions and Automation in Design, Vol. 110, pp. 397-404.
10. Stewart D., 1965, "A Platform with Six Degrees of Freedom", Proceedings of Institute of Mechanical Engineering, London England, Vol. 180, pp. 371-386.
11. Tahmasebi F., Tsai L.W., 1994, "Closed-Form Direct Kinematics Solution of a New Parallel Minimanipulator", Transactions of the ASME, Vol. 116, pp. 1141-1147.
12. Tsai L.W., Tahmasebi F., 1983, "Synthesis and Analysis of a New Class of Six Degree-of-Freedom Parallel Minimanipulators", Journal of Robotic Research, Vol. 10, pp. 561-580.
13. Yang D.C., and Lee T.W., 1984, "Feasibility Study of a Platform Type of Robotic Manipulator from a Kinematic Viewpoint", ASME Journal of Mechanisms, Transmissions and Automation in Design, Vol. 106, pp. 191-198.